

Minimum energy state of the one-dimensional Coulomb chain

Daniel H. E. Dubin

Department of Physics, University of California at San Diego, La Jolla, California 92093-0319

(Received 17 October 1996)

One-dimensional chains of laser-cooled ions have recently been confined in the fields of electromagnetic traps. This paper considers the minimum energy states of this one-dimensional (1D) form of condensed matter. Molecular dynamics simulations of the minimum energy states are compared to a density functional theory of the inhomogeneous crystal. Unlike 2D and 3D inhomogeneous Coulombic systems, where mean-field theory works well in describing the overall density variation on scales large compared to an interparticle spacing, we show that correlations are essential in determining the density of the 1D Coulomb chain. On the other hand, the long-range interactions that contribute to the mean field must also be kept. [S1063-651X(97)02204-6]

PACS number(s): 64.70.-p, 61.50.-f

I. INTRODUCTION

The one-dimensional Coulomb chain is a form of condensed matter that consists of charges of like sign trapped along a linear axis through the application of strong external focusing fields. One-dimensional (1D) Coulomb chains consisting of up to several dozen ions have recently been created in experiments [1,2]. Interparticle separations, on the order of micrometers, are sufficiently large so that a classical description of the dynamics is valid in most experiments. The 1D chain has been suggested as an advantageous configuration for a novel type of atomic clock [3,4], as well as for quantum computer schemes [5].

In this paper we consider the equilibrium properties of the 1D Coulomb chain. We focus on the zero-temperature classical limit, where the particles are trapped at equilibrium positions along the chain axis. This limit has been approached in experiments by application of laser cooling. The equilibrium positions are determined by force balance between the mutual Coulomb repulsion of the like-sign charges and the external focusing fields. For a finite length chain confined by some external potential $\phi_e(z)$, the interparticle spacing varies with position z along the chain. In this paper we devise a theory that explains this variation.

These 1D inhomogeneous crystals have a unique property that distinguishes them from other common forms of condensed matter: correlation energy and mean-field energy are of the same order of magnitude; neither can be neglected when determining the equilibrium. Neglecting correlations is equivalent to replacing the N charges by a charged mean-field fluid (the correlation energy is the extra energy associated with the discreteness of the individual charges, and this energy is neglected in the mean-field approximation). However, the energy of a uniform line charge is infinite: there is no mean-field approximation for the 1D Coulomb chain. In order to obtain a finite energy the discreteness of the individual charges must be taken into account, so one cannot neglect correlations.

To see this another way, note that the energy of a D -dimensional Coulombic system of size L scales roughly as $q^2 N^2/L$. This estimate follows from considering long-range interactions between particles separated by a distance of order L ; there are roughly N^2 pairs of such particles. On the

other hand, correlation energy scales as $Nq^2/a = q^2 N^{1+1/D}/L$ where $a = (L^D/N)^{1/D}$ is the average interparticle spacing. For a system of dimension $D > 1$ and $N \gg 1$ one can see that the correlation energy makes a relatively small contribution so the energy is dominated by long-range interactions (i.e., the mean field). This is the familiar case in plasma physics—the density variation of an inhomogeneous 2D or 3D plasma is determined almost entirely by the mean field, with correlations affecting the density only on scales of order the interparticle spacing. However, for dimension $D = 1$ the correlation energy is of the same order as the mean-field energy arising from long-range interactions; neither can be neglected. We will see that for 1D Coulomb chains the correlations influence the density on all scales up to the system size.

This argument can be generalized to potentials other than Coulombic. For example, for potentials which are of inverse power form $1/r^n$ at long range, the analogous argument shows that correlation energy dominates over the mean-field energy arising from long-range interactions when $D < n$, whereas mean-field energy dominates over correlations in the opposite case $D > n$. In three dimensions mean-field energy and correlation energy are of the same order when $n = 3$. Seen in this light, this paper can be regarded as a specific example of the more general problem of determining equilibrium properties when both correlations and mean-field effects are equally important, applied to the physically interesting case of Coulomb interactions in one dimension.

We will account for correlations using a one-dimensional version of the local density approximation (LDA) [6]. In the LDA one approximates the correlation energy of the inhomogeneous system by an integral over the correlation energy of a homogeneous system. The approximation works well when the number of charges N is large and the interparticle spacing varies slowly with position.

In Sec. II we develop a general expression for the energy of a Coulomb chain as a functional of the chain density $n(z)$, i.e., the number of particles per unit length (the inverse of the interparticle spacing). In Sec. III we minimize this functional in order to determine the energy of the chain and the density as a function of position z . The results are compared to molecular dynamics simulations of the 1D chain. An asymptotic expression for the density of the chain is derived, valid for

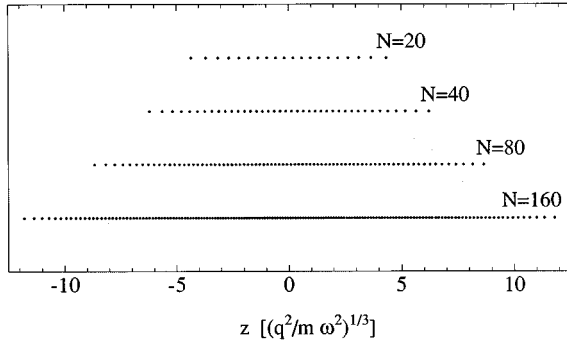


FIG. 1. Coulomb chains confined by a quadratic potential for different values of the particle number N . The position z of each ion is scaled to $(q^2/m\omega^2)^{1/3}$.

large N . The lowest-order asymptotic form applies even when surrounding conductors are present, and shows that image charges have only a small effect on the chain density. In Sec. IV we examine the approximations inherent in the LDA and consider an improvement to the LDA called the square-gradient approximation. In Sec. V we discuss our results.

II. LOCAL DENSITY APPROXIMATION

Consider a collection of N like charges, confined along the z axis at positions z_i , $i = 1, \dots, N$, by an external potential $\phi_e(z)$.

Note that we need not specify the form of ϕ_e as a function of the transverse coordinates x and y ; symmetry implies that only the z dependence of ϕ_e is needed when considering the chain equilibrium. (We say nothing here concerning stability of this equilibrium to transverse motions; see Refs. [7,8] for a discussion of stability.) The potential energy of this system is

$$E = \sum_{i>j}^N q^2 G(z_i, z_j) + \sum_i q \phi_e(z_i), \quad (1)$$

where $G(z_i, z_j)$ is the Green's function for the electrostatic potential (multiplied by -4π) including the effects of surrounding conductors, if any. The equilibrium positions can be determined by minimization of E with respect to the z_i 's, which can be easily performed numerically provided that N is not too large. Some results are displayed in Fig. 1, neglecting image charge effects so that $G = 1/|z_i - z_j|$, and choosing for the external potential a quadratic well:

$$q \phi_e(z) = \frac{1}{2} m \omega^2 z^2, \quad (2)$$

where m is the mass of a charge and ω is the oscillation frequency associated with the potential.

Two observations are immediately apparent: the Coulomb chains depicted in Fig. 1 are inhomogeneous; that is, the interparticle spacing a depends on position; and this dependence is smooth as a function of z .

We define the interparticle spacing $a(\hat{z}_i)$ at positions

$$\hat{z}_i = \frac{z_i + z_{i+1}}{2} \quad (3)$$

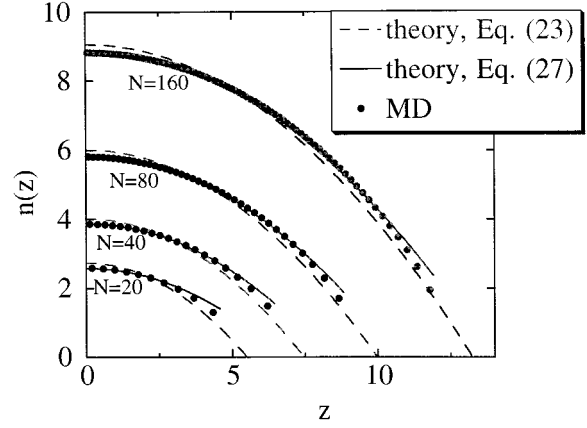


FIG. 2. Density per unit length, n , as a function of position z . Dots: $n(z_i)$ determined by MD simulation, where z_i is the position of the i th charge. Lines: method of trial variational functions. Dashed lines: one-parameter function [Eq. (23)]; solid lines: two-parameter function [Eq. (27)]. Both z and $n(z)$ scaled to $(q^2/m\omega^2)^{1/3}$.

as

$$a(\hat{z}_i) = z_{i+1} - z_i. \quad (4)$$

The inverse of this function,

$$n(\hat{z}_i) = a^{-1}(\hat{z}_i), \quad (5)$$

is the density of particles per unit length along the Coulomb chain. Figure 2 indicates that this density displays a smooth dependence on z . In Fig. 2 we have actually plotted $n(z_i)$, rather than $n(\hat{z}_i)$ where $n(z_i)$ is determined by interpolation of $n(\hat{z}_i)$. (Plotting the density evaluated at the actual particle positions gives one a better feel for the actual length of the chain.)

One goal of this section will be to attain some analytic understanding of how the density $n(z)$ varies. We will construct an approximate expression for the energy E of the system that depends on $n(z)$. Functional minimization of E with respect to $n(z)$ then will determine how the density varies.

For example, the term involving the external potential can be approximated by an integral over $n(z)$ when N is large and $n(z)$ varies slowly:

$$\Phi_e = \sum_{i=1}^N q \phi_e(z_i) \approx q \int_{-\infty}^{\infty} dz n(z) \phi_e(z). \quad (6)$$

$\Phi_e[n]$ is a functional of $n(z)$ that determines the potential energy due to the external potential.

We also require an integral expression for the Coulomb self-energy $\sum_{i>j} q^2 G(z_i, z_j)$. To this end, consider the self-potential-energy Φ of a globule of uniform fluid with density $\rho(r, z)$, chosen such that

$$\rho(r, z) = \begin{cases} \rho_0, & r < r_0(z) \\ 0, & r > r_0(z) \end{cases} \quad (7)$$

where ρ_0 is a constant density. The radius $r_0(z)$ and density ρ_0 of the globule are chosen so as to match the number per unit length $n(z)$:

$$\pi r_0(z)^2 \rho_0 = n(z). \quad (8)$$

The self-potential-energy of the globule is

$$\Phi = \frac{q}{2} \int \rho(r, z) \phi(r, z) d^3 \mathbf{r}, \quad (9)$$

where ϕ is the electrostatic potential, a solution to Poisson's equation

$$\nabla^2 \phi = -4\pi q \rho(r, z). \quad (10)$$

In the Appendix we show for a long thin globule for which

$$\frac{dr_0(z)}{dz} \ll 1 \quad \text{and} \quad r_0(z) \ll D. \quad (11)$$

where D is the distance to surrounding (if any), that Φ can be expressed in terms of $n(z)$ and $r_0(z)$ as a double integral over z :

$$\Phi = q^2 \int_{-\infty}^{\infty} dz \left[\frac{n(z)^2}{4} - \frac{n(z)}{2} \int_0^{\infty} dy \ln \left(\frac{2y}{r_0(z)} \right) \frac{\partial}{\partial y} \right. \\ \left. \times \{y[n(z-y)G(z, z-y) + n(z+y)G(z, z+y)]\} \right]. \quad (12)$$

One might hope that minimization of $\Phi + \Phi_e$ with respect to $n(z)$ would provide a well-defined result for $n(z)$. However, the result depends on $r_0(z)$, and in fact $\Phi \rightarrow \infty$ as $r_0(z) \rightarrow 0$, since a line charge has infinite self-energy.

In physical terms, the number of particles per unit length in a fluid globule depends not only on the confining force along the z axis, but also on the radial confining force. As one increases the radial confining force in order to shrink the globule onto the z axis, the globule will become longer and longer in z without limit. We therefore cannot use Eq. (12) alone to determine the density per unit length $n(z)$ of the Coulomb chain.

As discussed in the Introduction, we also need to account for correlations, which are neglected in Eq. (12). In order to account for correlations we add and subtract Φ from the exact energy E given by Eq. (1), using Eq. (6) for the external potential energy:

$$E = \Phi + \Phi_e + U, \quad (13)$$

where

$$U = q^2 \sum_{i>j} G(z_i, z_j) - \Phi. \quad (14)$$

Now, U is the difference between the exact Coulomb self-energy of the chain, and the energy of a uniform fluid globule with the same density per unit length, so U is an expression for the correlation energy of the system. We will now obtain an approximate form for the correlation energy U which is valid when Eq. (11) holds.

Suppose that the Coulomb chain is infinitely long and homogeneous in z . Then U is the difference between the energy of the chain and that of a uniform density cylinder. The correlation energy U^{hom} for this homogeneous system can be determined analytically (see Refs. [8,9]):

$$\frac{U^{\text{hom}}}{N} = q^2 n \left[\gamma - \frac{1}{4} + \ln \left(\frac{nr_0}{2} \right) \right], \quad (15)$$

where γ is Euler's constant. Provided that n and r_0 are slowly varying, we can employ Eq. (15) to find U for a nonuniform system in the local density approximation:

$$U = \int_{-\infty}^{\infty} dz n(z) \frac{U^{\text{hom}}}{N}(n) \quad (16)$$

or, substituting from Eq. (15),

$$U = q^2 \int_{-\infty}^{\infty} dz n^2(z) \left[\gamma - \frac{1}{4} + \ln \left(\frac{n(z)r_0(z)}{2} \right) \right]. \quad (17)$$

Note that the correlation energy depends logarithmically on r_0 . However, when Φ and U are added together to obtain an expression for E in Eq. (13), the dependence on r_0 vanishes and the energy depends only on the density per unit length:

$$E[n] = \int_{-\infty}^{\infty} dz n(z) \left\{ q^2 \gamma n(z) - \frac{q^2}{2} \int_0^{\infty} dy \ln[yn(z)] \frac{d}{dy} \right. \\ \left. \times [yn(z-y)G(z, z-y) + yn(z+y)G(z, z+y)] \right. \\ \left. + q\phi_e(z) \right\}. \quad (18)$$

Here we have used the fact that $\lim_{z' \rightarrow z} G(z, z') = 1/|z - z'|$, and have performed an integration by parts.

Equation (18) is the main result of this paper. In the next section we minimize $E[n]$ in order to determine the energy E and density $n(z)$ of the chain. However, before we do so, it may be instructive to evaluate Eq. (18) for a particular case that can be compared to an exact result. For a Coulomb chain of finite length and uniform interparticle spacing a_0 , the Coulomb self-energy is

$$E = \frac{q^2}{a_0} \sum_{i=1}^N \sum_{j=1}^{i-1} \frac{1}{|i-j|} \quad (19)$$

(we neglect the external potential and image charges for simplicity). The sums can be performed explicitly for large N [10]:

$$E = \frac{q^2}{a_0} (N-1) \left[\gamma - 1 + \ln(N-1) + O\left(\frac{\ln N}{N}\right) \right]. \quad (20)$$

Let us compare this result to Eq. (18). A uniform chain of N charges has length $a_0(N-1)$ and density a_0^{-1} so, neglecting image charges, Eq. (18) becomes

TABLE I. Energy of Coulomb chains in a quadratic well [in units of $m\omega^2(q^2/m\omega^2)^{2/3}$].

N	$E_{\text{simulation}}$	$E(N)^{\text{a}}$	$E(N)^{\text{b}}$	$E(N)^{\text{c}}$	$E(N)^{\text{d}}$
20	180.3	181.1	179.8	180.1	179.8
40	665.76	665.84	665.27	665.6	665.3
80	2389.71	2 393.9	2 389.2	2389.8	2 389.2
160	8414.2	8 424.6	8 413.9	8414.2	8 413.53
1 280		342 063.1	341 913.3		341 876.50
5 000		3 735 837.1	3 734 872.7		3 734 469.71
10 000		12 513 080.7	12 510 529.8		12 509 232.82

^aEquation (26).

^bNumerical minimization of Eq. (29) (same as $M=2$ in Table II).

^cBest value, full numerical minimization, finite-difference method.

^dBest value, full numerical minimization, Legendre expansion method (from Table II).

$$E(n) = q^2 \int_0^{a_0(N-1)} dz \left\{ \gamma a_0^{-2} - \frac{a_0^{-1}}{2} \right. \\ \left. \times \left[\int_0^\infty dy \ln(y a_0^{-1}) \frac{d}{dy} [n(z-y) + n(z+y)] \right] \right\}. \quad (21)$$

The derivatives of $n(z \pm y)$ create δ functions at the chain ends, so the integral over y can be evaluated, after which the z integral can be performed, yielding

$$E = \frac{(N-1)q^2}{a_0} [\gamma - 1 + \ln(N-1)]. \quad (22)$$

This matches Eq. (20) to $O(\ln N/N)$. When an external potential is added we will see in the next section that the energy functional also matches simulation results for the minimum energy state to high accuracy.

III. DETERMINATION OF THE COULOMB CHAIN DENSITY AND ENERGY IN THE LDA

In this section we minimize $E[n]$ using several different techniques. First, we employ trial variational functions in order to obtain analytic estimates for the energy and density of the chain. Next, we consider a full numerical minimization of the energy functional using two numerical techniques: expansion of $n(z)$ in basis functions, and finite differencing. Finally, we consider the limit of large N and analytically expand the variational solution for $n(z)$ in powers of $1/(\ln N)$. In each case we compare the results to molecular dynamics (MD) simulations. For simplicity image charge effects are neglected throughout, except in Sec. III C.

A. The method of trial variational functions

An approximate minimization of Eq. (18) can be accomplished by choosing an appropriate variational function for $n(z)$ whose shape depends on one or more independent parameters. The energy can then be minimized with respect to these parameters.

We will neglect image charges and assume a harmonic potential of the form given by Eq. (2). In this case

$$G(z, z \pm y) = \frac{1}{|y|}.$$

One straightforward choice for $n(z)$ that works reasonably well involves a single parameter L [8]:

$$n(z) = \begin{cases} \frac{3}{4} \frac{N}{L} \left(1 - \frac{z^2}{L^2} \right), & |z| < L \\ 0, & \text{otherwise,} \end{cases} \quad (23)$$

L being the half length of the chain. The required integrals in $E[n]$ can then be performed analytically, yielding

$$E = \frac{1}{10} N m \omega^2 L^2 + \frac{3}{5} \frac{q^2 N^2}{L} \left[\gamma - \frac{13}{5} + \ln(6N) \right]. \quad (24)$$

Minimization of E with respect to L provides a relation between L and N :

$$L^3(N) = 3 \frac{q^2 N}{m \omega^2} \left(\gamma - \frac{13}{5} + \ln(6N) \right), \quad (25)$$

and use of this relation in Eq. (24) implies that the energy of the chain is

$$E(N) = \frac{3}{10} N m \omega^2 L^2(N). \quad (26)$$

For various N values $E(N)$ is compared to the simulation results in Table I, and the density is compared to the simulation in Fig. 2. The energies are close, but are slightly larger than the simulation results, and the length of the chain is slightly overestimated, although as N increases the percentage error decreases (slowly).

An improved fit to the simulation results can be achieved by using a more flexible trial variational function,

$$n(z) = \begin{cases} A - Bz^2, & |z| \leq L \\ 0, & |z| > L. \end{cases} \quad (27)$$

The constraint that $\int_{-L}^L n(z) dz = N$ implies a relation between the parameters A , B , and L :

$$2L(A - BL^2/3) = N, \quad (28)$$

so there are actually two independent variational parameters, as opposed to only one in Eq. (23).

The integrals in Eq. (18) can be performed analytically, yielding the following result for $E[n]$:

$$E = q^2 L \left\{ -\frac{62}{15} A^2 + L^2 \left[\frac{m\omega^2}{q^2} \left(\frac{A}{3} - \frac{BL^2}{5} \right) + \frac{12}{5} AB - \frac{26}{25} B^2 L^2 \right] + \frac{32 A^2}{15 L} \sqrt{A/B} \tanh^{-1}(\sqrt{B/AL}) + \left(2A^2 - \frac{4AB}{3} L^2 + \frac{2B^2 L^4}{5} \right) \{ \gamma + \ln[2L(A - BL^2)] \} \right\}. \quad (29)$$

(To obtain this result one must take into account the density discontinuities at $z = \pm L$, which create δ functions in the derivative of n .)

Equation (29) can be minimized numerically for a given value of N by substituting for A in terms of N , B , and L via Eq. (28), and minimizing with respect to B and L . Results for the energy are displayed in Table I, and the density is compared to the simulations in Fig. 2. There is a considerable improvement in the fit compared to the one-parameter variational function of Eq. (23).

One might imagine that by choosing even more flexible trial functions with more variational parameters, one could further improve the accuracy of the fit. However, as we will see in the next section, this is true only up to a certain point, since the convergence of the theory to the true energy and density turns out to be ‘‘asymptotic.’’ By this we mean that a series of increasingly flexible variational functions converges only up to a certain point, beyond which the results for $n(z)$ and E diverge. However, we will see that as N increases, more terms in the series can be kept before loss of convergence, and for large N it is possible to determine the energy and the density to high accuracy.

B. Numerical minimization of $E[n]$

In order to numerically minimize $E[n]$, we first assume that $n(z)$ is nonzero only for $|z| \leq L$, where L is the half length of the chain, a parameter to be determined during the minimization procedure. We write $E[n]$ in terms of $\bar{z} = z/L$, $\bar{y} = y/L$, and $\bar{n} = n(q^2/m\omega^2)^{1/3}$ where $(q^2/m\omega^2)^{1/3}$ is a scale length associated with the harmonic potential:

$$E = \frac{2q^2 \bar{L}}{(q^2/m\omega^2)^{1/3}} \int_0^1 d\bar{z} \bar{n}(\bar{z}) \left(\bar{n}(\bar{z}) \{ \gamma + \ln[\bar{n}(\bar{z}) \bar{L}] \} + \frac{1}{2} \int_0^{1+\bar{z}} d\bar{y} \ln(\bar{y}) \bar{n}'(\bar{z} - \bar{y}) - \frac{1}{2} \int_0^{1-\bar{z}} d\bar{y} \ln(\bar{y}) \bar{n}'(\bar{z} + \bar{y}) + \frac{1}{2} \bar{L}^2 \bar{z}^2 \right), \quad (30)$$

and where $\bar{L} = L/(q^2/m\omega^2)^{1/3}$ and $\bar{n}'(\bar{z}) = \partial \bar{n} / \partial \bar{z}$. Here again we have neglected image charges so that $G(z, z \pm y) = 1/|y|$ and we have assumed the trap is harmonic for simplicity.

The scaled half length \bar{L} is determined by the condition that the number of charges remains fixed during the minimization procedure:

$$\bar{L} = N \int_{-1}^1 d\bar{z} n(\bar{z}). \quad (31)$$

We first perform the numerical minimization by means of a finite-difference scheme. We replace the function $n(z)$ by the set of discrete values $n(z_i)$, $\bar{z}_i = i/M$, $i = 0, 1, 2, \dots, M$. In order to speed up the numerics we use the symmetry of the harmonic well to assume $n(-\bar{z}) = n(\bar{z})$, and we also assume $n(1) = 0$. The integral over \bar{z} is then performed using the corrected composite trapezoid rule:

$$\int_0^1 f d\bar{z} = \frac{1}{M} \left(\sum_{i=1}^{M-1} f(\bar{z}_i) + \frac{1}{2} [f(0) + f(1)] + \frac{1}{12M} [f'(0) + f'(1)] \right), \quad (32)$$

where $f(\bar{z})$ is the integrand in Eq. (30). Since symmetry implies $n'(0) = 0$, one can show that $f'(0) = 0$; and $n(1) = 0$ implies $f(1) = 0$. We replace $f'(1)$ by its finite-difference form, $f'(1) = [f(1) - f(\bar{z}_{M-1})]M = -f(\bar{z}_{M-1})M$.

We must also finite difference the integrals over \bar{y} that enter into $f(\bar{z})$. For those integrals we employ the uncorrected composite trapezoid rule,

$$\int_0^{1 \pm \bar{z}_i} g(\bar{y}) d\bar{y} = \frac{1}{M} \left(\sum_{j=1}^{M \pm i - 1} g(\bar{y}_j) + \frac{1}{2} [g(0) + g(1 \pm \bar{z}_i)] \right), \quad (33)$$

where $g = \ln \bar{y} n'(\bar{z}_i \pm \bar{y})$, noting that the logarithmic divergence in $g(0)$ vanishes through a cancellation between the two integrals over \bar{y} . The derivative of n is evaluated using the midpoint rule:

$$n'(z_i) = \frac{n(\bar{z}_{i+1}) - n(\bar{z}_{i-1})}{2(1/M)}, \quad i = 1, \dots, M-1$$

$$n'(0) = 0,$$

$$n'(1) = -n(\bar{z}_{M-1})/(1/M). \quad (34)$$

For a given number of charges N there are M variational parameters, $n(\bar{z}_i)$, $i = 0, \dots, M-1$. Minimization of $E[n]$ with respect to these M parameters can be performed using any numerical minimization routine.

Results for the energy as a function of M are displayed in Fig. 3 for $N = 20, 40, 80$, and 160 charges. As M increases, the energy is observed to converge to a value which is a good match to the simulation results (see Table I); however, when M becomes too large the energy begins to diverge. As N increases, the range of M over which energy converges increases, and the energy can be determined to more significant figures. The loss of convergence is a common problem in local density approximations of Coulombic systems, and is related to the onset of oscillations in the density. These oscillations can be observed in Fig. 4 for $N = 20$ and 40, which displays the density as a function of position com-

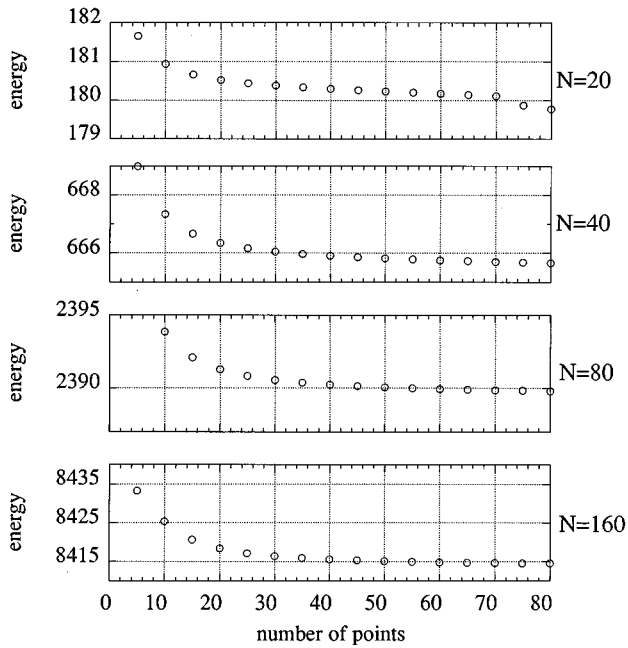


FIG. 3. Energy as a function of the number of points M kept in the finite-difference method for $N=20, 40, 80,$ and 160 . Energy in units of $m\omega^2(q^2/m\omega^2)^{2/3}$.

pared to the MD simulations. For $N=20$ and 40 we also plot the density for the values of M that gives the best fit, $M=40$ and 60 , respectively. For $N=80$ and 160 no oscillations in the density are apparent because M is not sufficiently large to have lost convergence ($M=80$ for these two N values). One can see that the fit improves as N increases.

Lest the reader think that the oscillations in $n(z)$ are related to a numerical instability in our finite-difference ap-

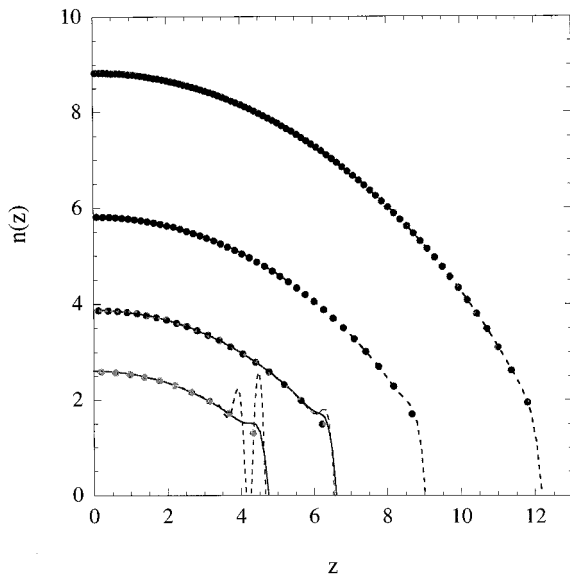


FIG. 4. Density as a function of position determined via the finite-difference method, compared to the MD simulations for $N=20, 40, 80,$ and 160 . Dashed lines: $M=80$. Solid lines are the values of M giving the best fit, $M=40$ for $N=20$ and $M=60$ for $N=40$. Both z and $n(z)$ scaled to $(q^2/m\omega^2)^{1/3}$.

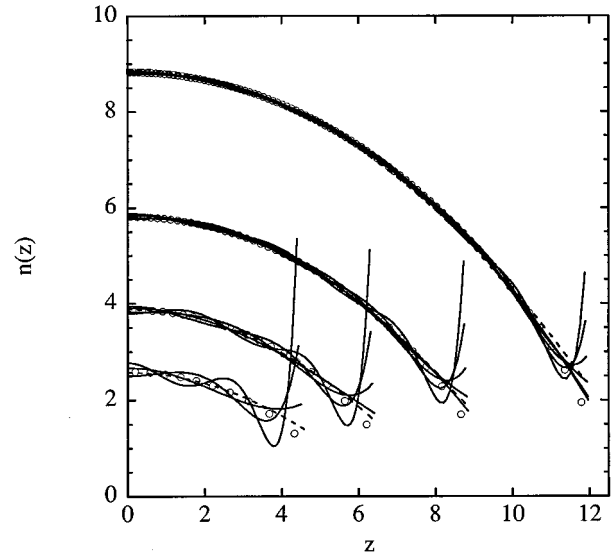


FIG. 5. Density as a function of position determined by the method of basis functions, compared to MD simulations (open circles) for $N=20, 40, 80,$ and 160 , keeping different numbers of basis functions: for $N=20, M=2-5$; for $N=40, M=2-6$; for $N=80, M=2-7$; for $N=160, M=2-8$. For each value of N the dashed curve corresponds to $M=2$ [same as Eq. (27)]. For $M \geq 3$ the different M values can be distinguished by noting that the density at $z=L$ increases as M increases. Both z and $n(z)$ scaled to $(q^2/m\omega^2)^{1/3}$.

proach rather than to a fundamental property of the density functional $E[n]$, we have also employed a second numerical minimization technique. In this approach we expand $\bar{n}(\bar{z})$ in the even Legendre polynomials:

$$\bar{n}(\bar{z}) = \sum_{m=0}^M A_m P_{2m}(\bar{z}). \quad (35)$$

The coefficient A_0 is determined by the normalization condition Eq. (31),

$$A_0 = \frac{N}{2L}, \quad (36)$$

so now there are $M+1$ variational parameters, A_1, A_2, \dots, A_M , and L . Minimization of Eq. (30) is aided by the fact that all of the required integrals over \bar{z} and \bar{y} (except for $\int_0^1 d\bar{z} \bar{n} \ln \bar{n}$) can be performed analytically. [Note that the case $M=1$ corresponds to the trial function of Eq. (27).]

Convergence to a limiting value of energy and density as M increases is quite rapid. However, if M becomes too large convergence is lost and oscillations in $\bar{n}(\bar{z})$ again ensue, just as in the finite-difference scheme (see Fig. 5). Indeed, when N is not large, the loss of convergence makes it difficult to determine the energy or the density beyond a certain accuracy. For example, when $N=160$, Table II implies $E=8413.5(\pm 0.1)$, and the density matches the MD simulation well, but for $N=20$ or 40 the energy does not converge to a very well-defined value, and neither does the density, as can be observed in Fig. 5.

However, the Legendre function technique is well suited to consideration of very large N values. We consider the

TABLE II. Energy [in units of $m\omega^2(q^2/m\omega^2)^{2/3}$] as a function of the number of basis functions M (best values in boldface).

M	$N=20$	$N=40$	$N=80$	$N=160$	$N=1280$	$N=5000$	$N=10\,000$
2	179.80	665.270	2389.189	8413.924	341 913.280	3 734 872.736	12 510 529.844
3	179.76	665.242	2389.173	8413.535	341 878.863	3 734 503.176	12 509 345.314
4	179.38	665.061	2389.099	8413.526	341 876.692	3 734 474.936	12 509 252.360
5	178.62	664.720	2388.923	8413.444	341 876.504	3 734 470.699	12 509 237.350
6		664.144	2388.636	8413.288	341 876.501	3 734 469.886	12 509 233.982
7			2388.200	8413.056	341 876.488	3 734 469.724	12 509 233.105
8				8413.728	341 876.444	3 734 469.706	12 509 232.875
9					341 876.369	3 734 469.706	12 509 232.826
10						3 734 469.694	12 509 232.822
11						3 734 469.664	12 509 232.821

cases $N=1280$, 5000 , and $10\,000$ in Table II. For $N=1280$ the value of M giving the best convergence is $M=6$, achieving eight figure accuracy in the resulting energy. When $N=10\,000$, ten significant figure accuracy in E is achieved for $M=11$ (the maximum value of M that our code allowed). The densities for these three cases are shown in Fig. 6 (on a logarithmic scale). Convergence to the limiting form may be seen here by plotting $n(\bar{z})$ for two values of M , the best value, and the best value minus one. Since there is no observable difference in $n(z)$ between the two M values, we may conclude that the densities shown have converged to the correct limiting form, even though there are no simulation data with which to compare since N is too large to perform simulations easily.

C. The large N limit of the LDA

It is possible to obtain some analytic results for $n(z)$ and $E(N)$ in the limit that $N \rightarrow \infty$. First we scale n , y , and z in the following manner:

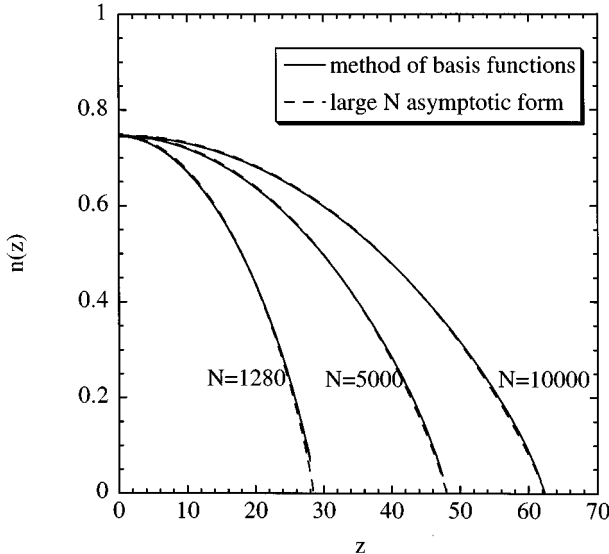


FIG. 6. Density as a function of z for $N=1280$, 5000 , and $10\,000$. Solid curves are the results of the method of basis functions. For each N value two values of M are plotted, the best value and the best value minus one (see text); the curves fall atop one another. Dashed curves correspond to the large N asymptotic form of Eqs. (48), (49a), and (53). $n(z)$ scaled to $N/L^{(0)}$ where $L^{(0)}$ is given by Eq. (47), and z scaled to $(q^2/m\omega^2)^{1/3}$.

$$\bar{z}=z/L, \quad \bar{y}=y/L, \quad \bar{n}=nL/N, \quad \bar{\phi}_e=\phi_eL/qN, \quad (37)$$

where L is the half length of the chain. Assuming the chain runs from $z=-L$ to L , so that $n(z)=0$ for $|z|>L$, and keeping image charge effects, the energy functional of Eq. (18) can be written as

$$E[n]=\frac{q^2}{L}\int_{-1}^1d\bar{z}\left(\bar{n}^2(\gamma+\ln N+\ln\bar{n})-\frac{\bar{n}}{2}\int_0^\infty d\bar{y}\ln\bar{y}\frac{d}{d\bar{y}}\right. \\ \left.\times[\bar{y}\bar{G}(\bar{z},\bar{z}+\bar{y})\bar{n}(\bar{z}+\bar{y})+\bar{y}\bar{G}(\bar{z},\bar{z}-\bar{y})\bar{n}(\bar{z}-\bar{y})]\right. \\ \left.+\bar{n}\bar{\phi}_e\right), \quad (38)$$

where $\bar{G}=LG$.

We will perform a variation keeping $\int n dz=N=\text{const}$, or

$$\int_{-1}^1\bar{n}d\bar{z}=1. \quad (39)$$

This variation is most easily performed by adding a Lagrange multiplier λ and minimizing the function

$$F[\bar{n}]=E[\bar{n}]-q^2\frac{\lambda}{L}\int_{-1}^1d\bar{z}\bar{n}. \quad (40)$$

The variational equation $\delta F/\delta\bar{n}(x)=0$ then implies

$$[2\gamma+1+2\ln\bar{n}+2\ln N]\bar{n}+\bar{\phi}_e-\lambda-\int_0^\infty d\bar{y}\ln\bar{y}\frac{d}{d\bar{y}} \\ \times[\bar{y}\bar{G}(\bar{z},\bar{z}+\bar{y})\bar{n}(\bar{z}+\bar{y})+\bar{y}\bar{G}(\bar{z},\bar{z}-\bar{y})\bar{n}(\bar{z}-\bar{y})]=0, \\ |\bar{z}|\leq 1 \quad (41a)$$

and this equation, along with the condition

$$\bar{n}(\bar{z})=0, \quad |\bar{z}|>1 \quad (41b)$$

determines the density.

We will solve Eq. (41) iteratively for \bar{n} in an expansion in $\ln N$. However, before we do so it is instructive to examine one feature of the solution following from Eq. (41): $\bar{n}(z)$ is

either continuous at $\bar{z}=\pm 1$, i.e., $\bar{n}(\pm 1)=0$, or else $\bar{n}(\pm 1)$ is singular. If $\bar{n}(z)$ is discontinuous at $\bar{z}=\pm 1$, the derivatives in Eq. (41a) imply that

$$\begin{aligned} & [2\gamma + 1 + 2 \ln \bar{n}_{\text{in}} + 2 \ln N] \bar{n}_{\text{in}} + \bar{\phi}_e - \lambda + \bar{n}_{\text{in}}(1)(1 - \bar{z}) \bar{G}(\bar{z}, 1) \\ & \times \ln(1 - \bar{z}) + \bar{n}_{\text{in}}(-1)(1 + \bar{z}) \bar{G}(\bar{z}, -1) \ln(1 + \bar{z}) \\ & - \int_0^{1+\bar{z}} d\bar{y} \ln \bar{y} \frac{d}{d\bar{y}} [\bar{y} \bar{G}(\bar{z}, \bar{z} - \bar{y}) \bar{n}_{\text{in}}(\bar{z} - \bar{y})] \\ & - \int_0^{1-\bar{z}} d\bar{y} \ln \bar{y} \frac{d}{d\bar{y}} [\bar{y} \bar{G}(\bar{z}, \bar{z} + \bar{y}) \bar{n}_{\text{in}}(\bar{z} + \bar{y})] = 0, \end{aligned} \quad (42)$$

where $\bar{n}_{\text{in}}(\bar{z})$ is the solution for $\bar{n}(\bar{z})$ when $|\bar{z}| \leq 1$. However, as $\bar{z} \rightarrow \pm 1$, the terms proportional to $\ln(1 \pm z)$ are singular, so $\bar{n}_{\text{in}}(\bar{z})$ is either infinite at $\bar{z} \rightarrow \pm 1$ or else $\bar{n}_{\text{in}}(\pm 1) = 0$.

We will focus on the nonsingular solutions for which $\bar{n}_{\text{in}}(\pm 1) = 0$. Under this restriction iterative solutions of Eq. (41) can be constructed. We have scaled the density so that it is of $O(1)$ as $N \rightarrow \infty$. The lowest-order solution to Eq. (41) is therefore

$$\bar{n}^{(0)}(\bar{z}) = \frac{\lambda - \bar{\phi}_e(\bar{z})}{2 \ln N}, \quad |\bar{z}| \leq 1. \quad (43)$$

The Lagrange multiplier is then determined by the condition Eq. (39), so the lowest-order solution for λ is

$$\lambda^{(0)} = \ln N + \langle \bar{\phi}_e \rangle / 2, \quad (44)$$

where $\langle \bar{\phi}_e \rangle = \int_{-1}^1 d\bar{z} \bar{\phi}_e(\bar{z})$. Thus to lowest order in $(\ln N)^{-1}$ the density is

$$\bar{n}^{(0)}(z) = \begin{cases} \frac{1}{2} - \frac{\bar{\phi}_e(\bar{z}) - \langle \bar{\phi}_e \rangle / 2}{2 \ln N}, & |\bar{z}| \leq 1 \\ 0, & |\bar{z}| > 1. \end{cases} \quad (45)$$

Note that $\bar{\phi}_e(\bar{z})$ depends on the half length L of the chain, which we have not yet determined. For example, for the harmonic potential

$$\bar{\phi}_e(\bar{z}) = \frac{m\omega^2}{2q^2} \frac{L^3 \bar{z}^2}{N}. \quad (46)$$

The length of the chain is determined by the condition that $\bar{n} = 0$ at $\bar{z} = \pm 1$. For the harmonic potential this condition together with Eqs. (45) imply that

$$L^{(0)3} = 3N \ln N \frac{q^2}{m\omega^2}, \quad (47)$$

the lowest-order solution for the half length of the chain. For this half length the density becomes

$$\bar{n}^{(0)} = \frac{3}{4} (1 - \bar{z}^2). \quad (48)$$

Note that Eq. (48) is equivalent to the trial function, Eq. (23), which explains why this trial function is a good choice for a plasma in a harmonic confinement potential.

Equations (45), (47), and (48) apply even when there are surrounding conductors that create image charge effects. Evi-

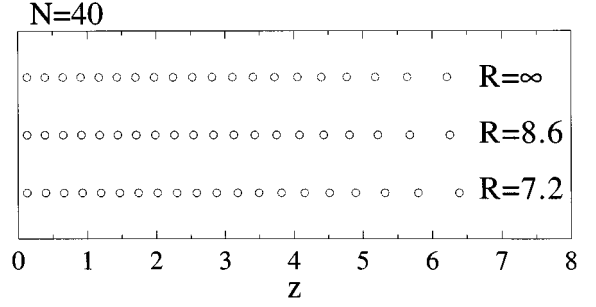


FIG. 7. Effect of image charges on equilibrium positions, for $N=40$. Right half of chain displayed. Spherical conductor, of radius R , centered at origin, is placed around the chain. Results for three values of R are shown. Distances are in units of $(q^2/m\omega^2)^{1/3}$.

ently image charges affect the 1D chain only at $O(1/\ln N)$. The effect of image charges on the 1D chain can be easily observed in MD simulations that include surrounding conductors. Figure 7 shows the equilibrium positions of 40 charges in a trap consisting of a harmonic external potential as well as a spherical conducting shell of radius R centered at the origin. The Green's function in this case is $G(z, z') = 1/|z - z'| - R/|R^2 - zz'|$. As one would expect intuitively, the charges are attracted to their images in the conductor, slightly lengthening the chain. However, even when R is only slightly larger than L the charge distribution is almost the same as the case $R = \infty$. This is different than for 2D or 3D plasmas, where the presence of nearby conductors would strongly distort the charge distribution.

Improvements to Eq. (48) can be made in an asymptotic series in powers of $(\ln N)^{-1}$. To next order, we write

$$\bar{n} = \bar{n}^{(0)} + \bar{n}^{(1)}, \quad (49a)$$

$$\lambda = \lambda^{(0)} + \lambda^{(1)}, \quad (49b)$$

$$L = L^{(0)} + L^{(1)}. \quad (49c)$$

The solution for $\bar{n}^{(1)}$ follows from Eq. (41a):

$$\begin{aligned} & 2 \ln N \bar{n}^{(1)} + [2\gamma + 1 + 2 \ln \bar{n}^{(0)}] \bar{n}^{(0)} + \bar{\phi}_e^{(1)} - \lambda^{(1)} \\ & - \int_0^{1+\bar{z}} d\bar{y} \ln \bar{y} \frac{d}{d\bar{y}} [\bar{y} \bar{G}(\bar{z}, \bar{z} - \bar{y}) \bar{n}^{(0)}(\bar{z} - \bar{y})] \\ & - \int_0^{1-\bar{z}} d\bar{y} \ln \bar{y} \frac{d}{d\bar{y}} [\bar{y} \bar{G}(\bar{z}, \bar{z} + \bar{y}) \bar{n}^{(0)}(\bar{z} + \bar{y})] = 0, \end{aligned} \quad (50)$$

where $\bar{\phi}_e^{(1)} = \bar{\phi}_e(\bar{Z})|_{L=L^{(0)}+L^{(1)}} - \bar{\phi}_e(\bar{Z})|_{L=L^{(0)}}$, or Taylor expanding,

$$\bar{\phi}_e^{(1)} = L^{(1)} \frac{\partial}{\partial L} \bar{\phi}_e(\bar{z})|_{L=L^{(0)}}. \quad (51)$$

Note that unless $\bar{n}^{(0)}(\pm 1) = 0$, $\bar{n}^{(1)}$ is infinite at $z = \pm 1$; as we discussed previously we therefore have chosen $\bar{n}^{(0)}(\pm 1) = 0$.

The Lagrange multiplier $\lambda^{(1)}$ is determined by Eq. (39), which implies

$$\int_{-1}^1 \bar{n}^{(1)} d\bar{z} = 0. \quad (52)$$

The correction to the half length $L^{(1)}$ is determined by the condition that $\bar{n}^{(1)}(\pm 1) = 0$.

For the harmonic potential of Eq. (46), and neglecting image charges, one can substitute Eq. (48) into Eq. (50) and perform the integrals analytically. After some work, and after applying the conditions $\bar{n}^{(1)}(\pm 1) = 0$, and Eq. (52) we obtain for the density

$$2(\ln N)n^{(1)} = \frac{3}{4}(1 - \bar{z}^2)[-5 + 6 \ln 2 - 3 \ln(1 - \bar{z}^2)], \quad (53a)$$

and for half length of the chain

$$(L^{(0)} + L^{(1)})^3 = \frac{3Nq^2}{m\omega_z^2} \left[\ln(6N) + \gamma - \frac{7}{2} + O\left(\frac{1}{\ln N}\right) \right]. \quad (53b)$$

Equation (53b) is similar to the expression for the half length, Eq. (25), derived using the trial function method. However, Eq. (53b) is a better (slightly shorter) approximation for the length, since it does not rely on an arbitrary choice for the form of a trial function. Equations (48) and (53) provide the asymptotic form for the density and length of the chain in a harmonic trap neglecting image charges. As an example we compare the asymptotic form for the density to the $N=1280$, 5000, and 10 000 data in Fig. 6, and we compare to the MD simulation for $N=160$ in Fig. 8.

Further improvements can be made by iterating the solution of Eq. (41) in order to keep even higher-order corrections to the density in powers of $(\ln N)^{-1}$. The iteration can be performed numerically, and we find that it provides excellent asymptotic convergence to the numerical simulations. For example, Fig. 8 shows the result keeping up to the sixth iterate, which is very close to the simulation results for $N=160$. However, as in the numerical work of Sec. III B, the convergence is only asymptotic: if too many iterates are kept the solution begins to oscillate.

IV. THE SQUARE-GRADIENT APPROXIMATION

In Eq. (18) the local density approximation was used in the energy functional. This approximation employs the correlation energy per particle of a homogeneous Coulomb chain, Eq. (15), in order to determine the correlation energy U of the inhomogeneous chain [see Eq. (16)]. To see what is left out in making this approximation, and how one might systematically improve on the LDA, consider an infinite Coulomb chain, initially homogeneous with density n_0 , to which is added a small density oscillation:

$$n(z) = n_0 + A \sin(kz), \quad (54)$$

where k is the wave number of the oscillation. We will determine the effect of this oscillation on the energy of the chain in two ways. First, we can determine the energy by expanding an exact expression for the chain energy in powers of A . Second, we will employ our energy functional, Eq. (18). Comparing these two results will tell us what the LDA has left out, and how we might improve on it.

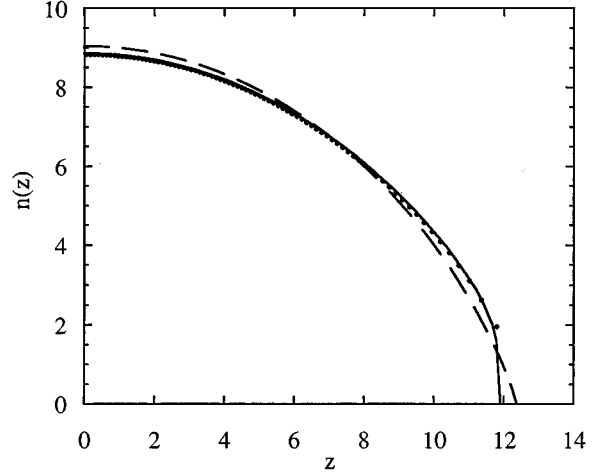


FIG. 8. Density as a function of z for $N=160$. Dots: MD simulation results. Dashed curve: large N asymptotic form [Eqs. (48), (49a), and (53)]. Solid curve: numerically iterated solution of Eq. (41), showing sixth iterate. Both z and $n(z)$ scaled to $(q^2/m\omega^2)^{1/3}$.

The exact Coulomb energy of the chain is

$$E = \sum_{\substack{i,j \\ j < i}} \frac{q^2}{|z(i) - z(j)|}. \quad (55)$$

Now, a small oscillation in the density of the chain is equivalent to an oscillation in the position of the particles. To be precise, for large N we can write a differential equation relating the density to the position $z(i)$ of particle i , based on Eqs. (3) and (5):

$$n(z) = 1/(dz/di). \quad (56)$$

Solution of this differential equation yields

$$i(z) = n_0 z \frac{A}{k} \cos(kz), \quad (57)$$

which can be inverted to obtain $z(i)$ to $O(A^2)$:

$$z(i) = a_0 i + \frac{A a_0}{k} \cos(ka_0 i) \left(1 - \frac{A}{k} \sin(ka_0 i) \right) + O(A^3), \quad (58)$$

where $a_0 = 1/n_0$ is the average interparticle spacing. To first order in A one can see that there is an oscillation in the interparticle spacing, as one would expect since the density is oscillating in z .

Using Eq. (58) in Eq. (55) and again expanding in A to quadratic order, one finds that for an infinite chain the terms linear in A cancel by symmetry and the energy is

$$E = E_0 + 2(N-1) \frac{q^2 A^2}{a_0^3 k^2} \sum_{j=1}^{\infty} \frac{\sin^2(ka_0 j/2)}{j^3}, \quad (59)$$

where E_0 is the energy of the uniform chain, given by Eq. (20) for large N . The $O(A^2)$ term is the potential energy associated with a phonon of wave number k .

Assuming that ka_0 is small, so that the wavelength of the inhomogeneity is long compared to an interparticle spacing, one can expand the sum in Eq. (59) to obtain

$$E = E_0 + 2(N-1)q^2 A^2 a_0 \times \left[\frac{1}{4} \left(\frac{3}{2} - \ln(ka_0) \right) + \frac{1}{144} \left(\frac{ka_0}{2} \right)^2 + \dots \right]. \quad (60)$$

We will now compare this expression to the expression obtained from Eq. (18). Substituting Eq. (54) into Eq. (18), and keeping only terms up to quadratic order in A , one performs the integrals over a chain of finite length $L = (N-1)a_0$. Then taking $L \rightarrow \infty$ and keeping only terms of $O(L)$ one finds that the energy is

$$E = E_0 + \frac{(N-1)}{2} q^2 A^2 a_0 \left(\frac{3}{2} - \ln(ka_0) \right). \quad (61)$$

Note that this expression, which employs the LDA, is nearly the same as the exact expression, Eq. (60), but misses the last term in the square brackets. This term, of $O(k^2)$, along with the other terms in the series of even higher order, is missing from the LDA. By keeping this $O(k^2)$ term in the energy we may improve the convergence of the energy functional to the actual energy. This extra energy can be expressed in terms of a derivative of the density:

$$\Delta E_{\text{SGA}} = \frac{q^2}{144} \int dz \left(\frac{1}{n} \frac{\partial n}{\partial z} \right)^2, \quad (62)$$

where we have kept terms only to lowest order in A . This extra energy is associated with variations in the density, and is similar to a term appearing in the energy of inhomogeneous fluids and referred to as the square-gradient approximation (SGA) or the van der Waals approximation [11]. In a fluid it provides an approximation to the interfacial energy due to surface tension. It is positive since surface tension always increases the energy of a stable interface.

Equation (61) shows that the LDA neglects terms proportional to gradients of the density. Thus, for slowly varying densities, the LDA is a good approximation, as expected. Also, adding Eq. (61) to the energy functional should help to suppress oscillations in the density that occurred in the LDA since such oscillations increase ΔE_{SGA} . However, the coefficient of $\frac{1}{144}$ in Eq. (61) is rather small, so we find that it does not stop the oscillations; it merely reduces their magnitude. An example is shown in Fig. 9 for the case of $N=20$ particles, a case for which oscillations are easily apparent in the LDA (see Fig. 4). We have added ΔE_{SGA} to the energy functional of Eq. (18) and have minimized the energy using the finite-difference method described in Sec. III B. As M increases the density oscillations are suppressed but not eliminated compared to Fig. 4, where only the LDA was employed in the energy functional. For larger values of N and for $M \lesssim 100$ the density in the SGA was found to be almost identical to the LDA results.

V. DISCUSSION

In order to describe the minimum energy states of inhomogeneous 1D Coulomb chains confined by external fields,

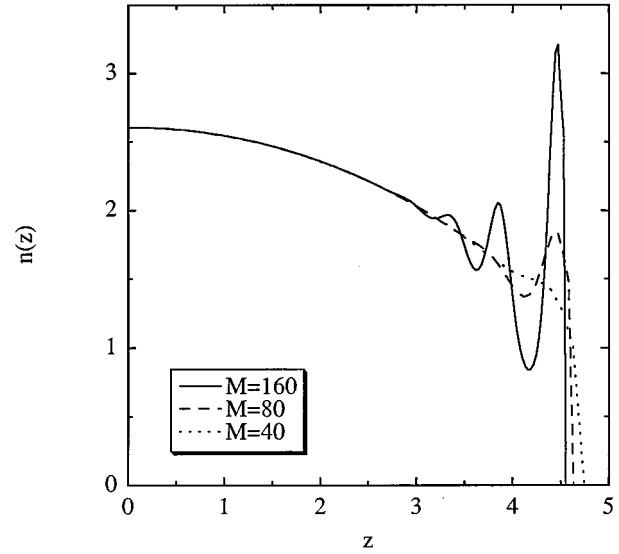


FIG. 9. Density as a function of z using the square-gradient approximation for $N=20$ and for three values of M . Both z and $n(z)$ scaled to $(q^2/m\omega^2)^{1/3}$.

we have developed an energy functional [Eq. (18)] based on the local density approximation. When minimized, this energy functional provides the energy and density per unit length as a function of position. The results were compared to molecular dynamics simulations and were found to be in good agreement with the simulations provided that the number of particles in the chain was sufficiently large. Of course, in present experiments a few dozen charges at most are trapped in the chain; and the determination of the equilibrium can be easily performed via molecular dynamics simulations such as those described in Sec. II. The density functional theory is valuable for $N \gg 1$, when MD simulations are difficult to perform. Such large chains may be realized in future experiments since some possible applications such as atomic clocks [3,4], quantum computers [5], and bunched crystallized beams in storage rings [12] appear to favor large N .

One-dimensional Coulombic matter was observed to have a property that distinguishes it from other Coulombic systems: both the mean-field and correlation energies must be kept when determining equilibrium properties; unlike 2D and 3D plasmas, correlation effects influence the density on scales large compared to an interparticle spacing. As a consequence, image charges due to surrounding conductors were shown to have only a small effect on the charge distribution of a 1D Coulomb chain. As we discussed in the Introduction, this balance between correlation and mean-field effects also occurs in higher-dimensional systems. In two dimensions the $1/r^2$ potential has this property, as does the $1/r^3$ potential in three dimensions.

In the future we intend to extend the present work to study finite-temperature effects in the 1D chains. Presumably the equilibrium density is affected by the pressure associated with random thermal motions of the particles, and a density functional theory based on minimization of free energy can be developed to describe this behavior.

ACKNOWLEDGMENTS

This work was supported by National Science Foundation Grant No. PHY94-21318 and Office of Naval Research Grant No. N00014-96-1-0239.

APPENDIX: MEAN-FIELD ENERGY OF A UNIFORM GLOBULE

In this appendix we evaluate a general expression for the mean-field self-energy of a uniform fluid globule of density ρ_0 . We assume that the globule is cylindrically symmetric and thin: its radius $r_0(z)$ is small compared to the distance to the surrounding electrodes, D , and slowly varying as a function of axial position z . The density and radius are chosen to equal a given number per unit length $n(z)$,

$$\pi r_0(z)^2 \rho_0 = n(z). \quad (\text{A1})$$

The electrostatic potential is then

$$\phi(r, z) = q\rho_0 \int_0^{2\pi} d\theta' \int_{-\infty}^{\infty} dz' \int_0^{r_0(z')} r' dr' G(\mathbf{r}, \mathbf{r}'). \quad (\text{A2})$$

We will eventually be interested in values of r and z within the globule, so $|z - z'|$ is much greater than both r and r'_0 except for a small range of z' values near z , $|z - z'| < \epsilon$ where

ϵ is a distance chosen such that $r_0(z) \ll \epsilon \ll D$. We therefore split the integral over z' into two parts; one running over $|z - z'| < \epsilon$ and one over $|z - z'| > \epsilon$:

$$\begin{aligned} \phi(r, z) = & q\rho_0 \int_0^{2\pi} d\theta' \int_{z-\epsilon}^{z+\epsilon} dz' \int_0^{r_0(z')} r' dr' G(\mathbf{r}, \mathbf{r}') \\ & + q\rho_0 \int_0^{2\pi} d\theta' \int_{-\infty}^{z-\epsilon} dz' \int_0^{r_0(z')} r' dr' G(\mathbf{r}, \mathbf{r}') \\ & + q\rho_0 \int_0^{2\pi} d\theta' \int_{z+\epsilon}^{\infty} dz' \int_0^{r_0(z')} r' dr' G(\mathbf{r}, \mathbf{r}'). \end{aligned} \quad (\text{A3})$$

In the last two integrals ϵ is sufficiently large so that we can replace $G(\mathbf{r}, \mathbf{r}')$ by $G(z, z')$, the Green's function evaluated along the z axis. The r' and θ' integrals can then be performed.

In the first integral in Eq. (A3), \mathbf{r} and \mathbf{r}' are sufficiently close together to neglect the conducting walls, and then we can approximate G by its vacuum form,

$$G(\mathbf{r}, \mathbf{r}') = \frac{1}{|\mathbf{r} - \mathbf{r}'|} = \frac{1}{\sqrt{(z - z')^2 + r^2 + r'^2 - 2rr' \cos \theta'}}.$$

The r' integral can then be done exactly. Putting together all three terms we have

$$\begin{aligned} \phi(r, z) = & q\rho_0 \int_0^{2\pi} d\theta' \int_{z-\epsilon}^{z+\epsilon} dz' \left[\sqrt{r^2 - 2rr'_0 \cos \theta' + r_0'^2 + (z - z')^2} - \sqrt{r^2 + (z - z')^2} \right. \\ & \left. + r \cos \theta' \ln \left(\frac{\sqrt{r^2 - 2rr'_0 \cos \theta' + r_0'^2 + (z - z')^2} + r'_0 - r \cos \theta'}{\sqrt{r^2 + (z - z')^2} - r \cos \theta'} \right) \right] \\ & + \pi q\rho_0 \left(\int_{z+\epsilon}^{\infty} dz' r_0'^2 G(z, z') + \int_{-\infty}^{z-\epsilon} dz' r_0'^2 G(z, z') \right), \end{aligned} \quad (\text{A4})$$

where $r'_0 = r_0(z')$ and $r_0 = r_0(z)$.

The integrals over θ and from $z - \epsilon$ to $z + \epsilon$ in the first term can be performed asymptotically in small ϵ [noting that r and r_0 are also of $O(\epsilon)$] and the result is

$$\phi(r, z) = \pi q\rho_0 \times \begin{cases} r_0^2(z) - r^2 + r_0^2 \ln 4\epsilon^2 / r_0^2 + \int_{\epsilon}^{\infty} dy [r_0^2(z+y)G(z, z+y) + r_0^2(z-y)G(z, z-y)], & r < r_0(z) \\ r_0^2 \ln 4\epsilon^2 / r^2 + \int_{\epsilon}^{\infty} dy [r_0^2(z+y)G(z, z+y) + r_0^2(z-y)G(z, z-y)], & r > r_0(z) \end{cases} \quad (\text{A5})$$

where we have made the replacements $y = z' - z$ and $y = z - z'$, respectively, in the last two integrals of Eq. (A4).

The integral over y is infinite as $\epsilon \rightarrow 0$ since $G(z, z \pm y) \rightarrow 1/|y|$ as $y \rightarrow 0$. However, the ϵ dependence can be canceled out by a mathematical trick. If one multiplies and divides by y in the integrand and then integrates by parts, a $\ln \epsilon$ term appears, canceling the $\ln \epsilon$ term in Eq. (A5). One can then take $\epsilon \rightarrow 0$ and obtain a finite result:

$$\phi(r, z) = \pi q\rho_0 \times \begin{cases} r_0^2(z) - r^2 - \int_0^{\infty} dy \ln \left(\frac{2y}{r_0(z)} \right) \frac{d}{dy} \{y[r_0^2(z-y)G(z, z-y) + r_0^2(z+y)G(z, z+y)]\}, & r < r_0 \\ - \int_0^{\infty} dy \ln \left(\frac{2y}{r} \right) \frac{d}{dy} \{y[r_0^2(z-y)G(z, z-y) + r_0^2(z+y)G(z, z+y)]\}, & r > r_0. \end{cases} \quad (\text{A6})$$

Note that the form of the potential as a function of r is the same as that of an infinite cylinder of radius r_0 : it is quadratic in r within the plasma and logarithmic outside the plasma. This form for the potential is valid only when both r and r_0 are small compared both to the gradient scale length of $r_0(z)$ and the distance to the electrodes.

Finally, the energy Φ of the globule follows from the general formula

$$\Phi = \frac{1}{2}q \int \rho \phi d^3r = \frac{1}{2}q\rho_0 2\pi \int_{-\infty}^{\infty} dz \int_0^{r_0(z)} r dr \phi(r, z).$$

Performing the r integral yields

$$\Phi = q^2 \int_{-\infty}^{\infty} dz \left[\frac{1}{4} n^2(z) - \frac{n(z)}{2} \int_0^{\infty} dy \ln\left(\frac{2y}{r_0(z)}\right) \frac{d}{dy} \{y[n(z-y)G(z, z-y) + n(z+y)G(z, z+y)]\} \right], \quad (\text{A7})$$

where we have employed Eq. (A1) to express $r_0^2(z)$ in terms of $n(z)$.

-
- [1] G. Birkel, S. Kassner, and H. Walther, *Nature (London)* **357**, 310 (1992).
 [2] M. G. Raizen *et al.*, *Phys. Rev. A* **45**, 6493 (1992).
 [3] W. M. Itano and N. F. Ramsey, *Sci. Am.* **269**, 59 (1993).
 [4] M. E. Poitzsch *et al.*, *Rev. Sci. Instrum.* **67**, 129 (1996).
 [5] J. I. Cirac and P. Zoller, *Phys. Rev. Lett.* **74**, 4091 (1995).
 [6] P. Hohenberg and W. Kohn, *Phys. Rev.* **136**, B864 (1964).
 [7] J. P. Schiffer, *Phys. Rev. Lett.* **70**, 818 (1993).
 [8] D. H. E. Dubin, *Phys. Rev. Lett.* **71**, 2753 (1993).
 [9] H. Totsuji, *Phys. Rev. A* **38**, 5444 (1988).
 [10] I. S. Gradshteyn and I. M. Ryzhik, *Table of Integrals, Series and Products* (Academic, New York, 1980), p. 7.
 [11] See, for example, R. Evans, *Adv. Phys.* **28**, 143 (1979); J. L. Leibowitz and J. K. Percus, *J. Math. Phys.* **4**, 116 (1963).
 [12] J. S. Hangst *et al.*, *Phys. Rev. Lett.* **74**, 4432 (1995).